AIP Advances

Magnetic plasmonic particles for SERS-based bacteria sensing: A review

Cite as: AIP Advances **9**, 010701 (2019); https://doi.org/10.1063/1.5050858
Submitted: 03 August 2018 . Accepted: 20 December 2018 . Published Online: 10 January 2019

Chaoguang Wang, Marco M. Meloni, Xuezhong Wu, Ming Zhuo, Taigang He, Junfeng Wang, Chongwen Wang, and Peitao Dong

AIP Advances ARTICLE scitation.org/journal/adv

Magnetic plasmonic particles for SERS-based bacteria sensing: A review

Cite as: AIP Advances 9, 010701 (2019); doi: 10.1063/1.5050858
Submitted: 3 August 2018 • Accepted: 20 December 2018 •
Published Online: 10 January 2019

View Online Export Citation CrossMark

Chaoguang Wang,[1,a),b)] Marco M. Meloni,[2,a)] Xuezhong Wu,[1] Ming Zhuo,[1] Taigang He,[2]
Junfeng Wang,[1] Chongwen Wang,[3] and Peitao Dong[1,b)]

AFFILIATIONS

[1] College of Mechatronics Engineering and Automation, National University of Defense Technology, Changsha 410073, China
[2] Molecular and Clinical Sciences Research Institute, St George's, University of London, London SW17 0RE, UK
[3] Key Laboratory of New Molecular diagnosis technologies for infectious diseases, Institute of Radiation Medicine, Academy of military medical sciences, Beijing 100850, China

[a)] **These authors contributed equally to this work.**
[b)] **Corresponding authors:** wangchaoguang@nudt.edu.cn; ptdong@nudt.edu.cn

ABSTRACT

This review describes recent advances in the use of magnetic-plasmonic particles (MPPs) for bacteria detection by Surface-Enhanced Raman Scattering (SERS). Pathogenic bacteria pollution has always been a major threat to human health and safety. SERS spectroscopy has emerged as a powerful and promising technique for sensitive and selective detection of pathogen bacteria. MPPs are considered as a versatile SERS platform for their excellent plasmonic properties and good magnetic responsiveness. Improved preparation method and typical characterization technique of MPPs are introduced, focusing on the thin and continuous metallic shell covering process. Consequently, the SERS-based sensing methods for bacteria identification were discussed, including the label-free and label-based methods. Finally, an overview of the current state of the field and our perspective on future development directions are given.

I. INTRODUCTION

Diseases caused by pathogenic bacteria remain a major threat to safety and health of human beings.[1] Pathogens present in food, water, or even in air often contain etiologic agents of many serious and even fatal diseases. Furthermore, some infectious disease bacteria can broaden the range of pathogen pollution and infect others. Rapid and accurate detection of pathogenic bacteria is therefore considered an effective way to save lives and reduce healthcare costs.[2,3] The current gold standard for pathogens testing in hospitals is based on strains culturing and growing, often known as colony counting method. Although reliable and sensitive, this technique suffers from a laborious and time-consuming process, usually up to 1~3 days, during which the most opportune time for diagnosis and treatment passes.[4–6] An alternative approach is to detect the specific gene of the pathogen instead of detecting the pathogen itself. Real time polymerase chain reaction (rtPCR) is recently preferred to identify the pathogens in DNAs sequences during their amplification, only taking 1~2 hours. However, professional kits, complex and careful procedures, specialized operators, and considerable time are required to extract the DNAs from the pathogens.[7–10] In addition to the laborious pretreatments, rtPCR method suffers from occasional fluorescence quenching, single-channel detection, and sophisticated equipment, as it acquires the fluorescence signals of the labels which are modified in the end of the DNA sequences. Therefore, there is great need to develop novel techniques which can detect the pathogens directly while reducing the assay time significantly.

Surface-enhanced Raman scattering (SERS) is a powerful and promising spectroscopy technique that can not only provide an ultra-sensitive characterization and analysis strategy up to molecular levels, but also produce the "fingerprint" messages of the target species.[11–13] These fascinating advantages have triggered extensive research on SERS technique as well as its potential applications in the fields of sensing,[14–16] biology assay,[17–20] and analytical chemistry.[21–24] For bacteria, the SERS-based sensing approaches are classified into two categories, namely the label-free and label-based methods.[25,26] The label-free approach detects bacterial pathogens without any label because each bacterial pathogen has an intrinsic SERS spectrum. The intrinsic SERS patterns originate from various components of the cell wall.[27–31] Simultaneous detection and identification of various pathogens is realized by analyzing the SERS spectra.[32] By contrast, the label-based approach employs a label, usually called SERS-tag,[25] to mark the pathogens. In this scenario antibodies and aptamers are often utilized to form a specific binding to the bacteria and construct a sandwich structure. The SERS signal of the SERS label reports the appearance of the bacteria through the specific bio-recognition. The schematic illustration of label-free and label-based SERS method for bacteria detection is shown in Fig. 1.

Both label-free and label-based sensing approaches rely on the SERS substrate's dramatic signal enhancement ability (10^5 to 10^{12}), which originates dominantly from the electromagnetic field concentration or coupling at the nanotips or nanogaps of the noble metal nanostructures. These areas with greatly enhanced electromagnetic field are called 'hotspots' for SERS and are used to amplify the usually weak Raman scattering signals. The fabrication of high-performance SERS substrate is a key factor for the bacteria detection. By now, SERS substrates or platforms were constructed generally by either solution-based nanoparticles (NPs) synthesis or solid-phase nanostructure (NS) fabrication.[33] The solid phase NS substrates, especially the ones with complicated morphologies, have received much attention due to the hotspots engineering at the tips and gaps. Several fabrication strategies have been developed to fabricate NS arrays including electron-beam lithography,[34,35] focused ion beam lithography,[36] nanoprint lithography,[37–39] nanosphere lithography (NSL),[40–52] glancing angle deposition technique,[53] metal annealing,[54] and silicon wet etching.[55–57] However, sophisticated equipment, tedious process, high cost, and poor biocompatibility of the solid phase substrate hamper its application in bioassay. The solution-synthesis-based NPs, such as Au/Ag NPs,[58,59] core-shell NPs,[11,60,61] self-gapped NPs,[62] and DNA connected dumbbells NPs[63,64] demonstrate remarkable signal enhancement ability, excellent biological compatibility, simple and cost-effective synthesis process. However, the NPs suspension have several drawbacks including the poor stability and difficulty in hotspots control.

As a novel SERS substrate, emerging magnetic-plasmonic particles (MPPs) have attracted increasing attention in recent years due to their excellent controllability and stability, though synthesized in solution. The magnetic core can be conveniently manipulated by the external magnet, which facilitates the process to separate the targets, replacing the usually used centrifugation process. The noble metal shell provides the hotspots in the SERS measurements. With advantages of good sensitivity, simple fabrication procedure, low cost and excellent controllability, MPPs demonstrate great potential and promise in SERS-based sensing, especially for rapid bacterial cell detection.

This review is mainly based on the work in our lab conducted in the past five years. A comprehensive literatures are included to provide an overview of current developments and trends in pathogen bacteria sensing with the aid of the MPPs as the SERS substrate. Firstly, we will give an overview of MPPs preparation methods and the typical characterization means.

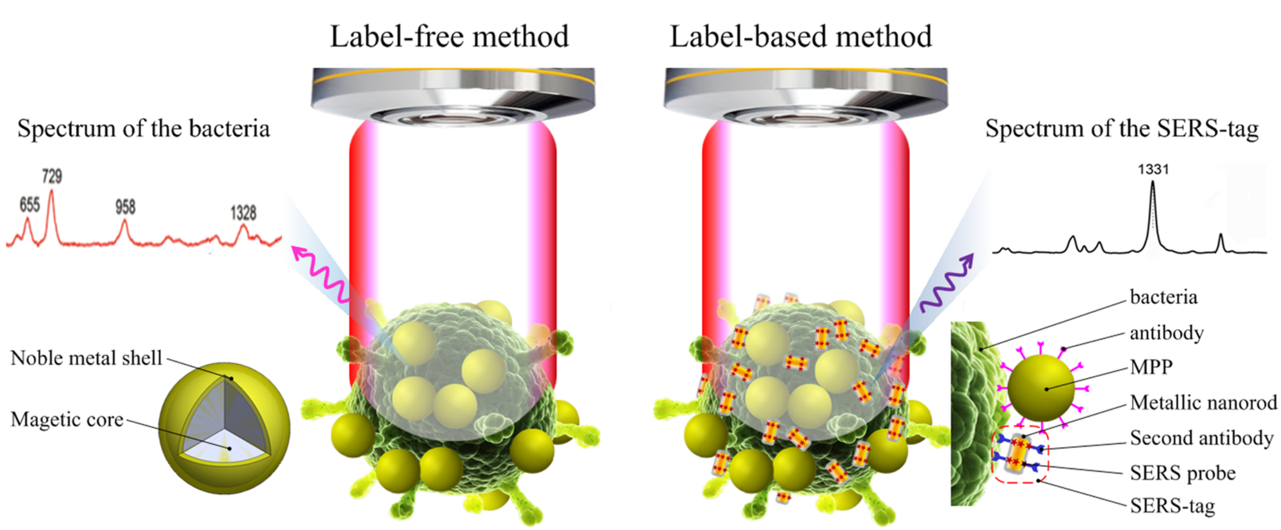

FIG. 1. Schematic illustration of label-free and label-based SERS method for bacteria detection.

Secondly, we will discuss the use of MPPs in bacteria detection with the label-free and label-based SERS sensing methods. For the label-based SERS sensing, typical immuno-assay and aptamer recognition sensing methods will be discussed separately. Finally, we will outline challenges and future perspectives in this evolving field, such as the sensing reproducibility, whole-organism fingerprinting database establishment, and parameters optimization.

II. MPPs PREPARATION AND CHARACTERIZATION

MPPs usually have a core-shell structure, with the magnetic core inside and the noble metal shell outside. The functionalized MPPs are generally prepared via three steps: the magnetic core synthesis, noble metal shell coating, and bio/chemical modification (Fig. 2a). The magnetic core, MFe_2O_4, is usually synthesized through a solvothermal reaction.[65–67] Herein, M represents the divalent metal ions, such as Fe^{2+}, Mn^{2+}, Zn^{2+}, Cu^{2+}, Ni^{2+}, Mg^{2+}, Co^{2+}. Then, the magnetic core is coated with a thin and continuous noble metal shell, such as Au and Ag, for outstanding SERS performance. To catch and enrich the target, the prepared MPPs is functionalized with chemical or biological molecules.

A. MPPs fabrication background

A myriad of synthetic methods have been proposed to prepare high-performance MPPs with good monodispersity, strong magnetic responsiveness, excellent SERS performance, and good biocompatibility. Zhong's group employed thermally activated processing protocol to prepare MPPs.[68,69] The particles obtained have a mean diameter of 6.3nm, which is too small to provide enough magnetic responsivity. These small AuMPs fabricated by Zhong's group are not sufficient for target separation, especially for the big bacterial cells. To fabricate bigger MPPs (diameter>100nm), the AuNPs were grafted directly to the magnetic core either by the chemical bonding[70] or the electrostatic interaction[71] to prepare Fe_3O_4-Au NPs composites. However, AuNPs cannot cover the magnetic core, which will evidently affect the composites' SERS performance. To obtain a continuous shell, silicon was employed as an interlayer for the metal shell formation. Ji's group coated the Fe_3O_4 core with a silica shell to facilitate deposition of gold seeds and reduction of K-gold solution with formaldehyde.[72] Han's group coated Ag shells on a Fe_3O_4@SiO_2 composite using a "seed–mediated growth" method.[73] Hu's group deposited AgNPs on surfaces of Fe_3O_4@SiO_2 composite by the Ag–mirror reaction.[74] However, the nonmagnetic silicon interlayer seriously affected the magnetic capability of the MPPs. Li's group developed a facile one-pot hydrothermal approach to synthesize Fe_3O_4@Au NPs.[75] The controllability of the process and the uniformity of the synthesized particles however need further improvements. Hydroxylamine seeding method can be utilized to synthesize AuMPs with uniform size and shape because of its separation of nucleation and growth stages.[76] Hydroxylamine or hydroxylamine hydrochloride can reduce chloroauric acid to elemental gold (Au^0) and gold particle surfaces can accelerate the occurrence of this reaction {Winkler, 2011 #6765}. Reduced Au^0 can be adsorbed on the surfaces of existing Au seeds, thus generating larger NPs rather than new nucleation. Lyon's group modified the hydroxylamine seeding procedure of Natan to synthesize AuMNPs for the first time and named the modified approach as iterative hydroxylamine seeding.[77] Based on Lyon's method, Zhou's group[78] and Gu's group[79] successfully synthesized cluster/shell Fe_3O_4/Au nanoparticles and Fe_2O_3/Au core/shell nanoparticles, respectively.

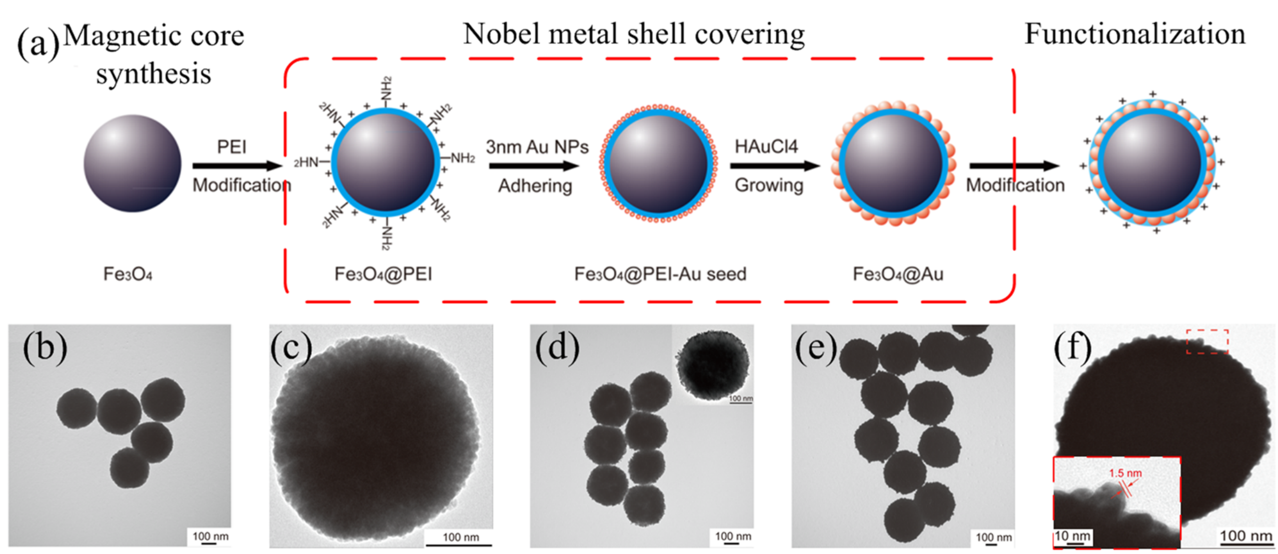

FIG. 2. (a) Schematic of the synthesis of functionalized MPPs and the TEM images for each MPPs preparation step, (b) Fe_3O_4 particles, (c) Fe_3O_4@PEI particle, (d) Fe_3O_4@PEI-AuNPs microspheres, (e) Fe_3O_4@Au particles, and (f) PEI modified Fe_3O_4@Au particles.

Although the iterative hydroxylamine seeding growth method has been widely used, its cumbersome and time-consuming route remains to be optimized.

B. Fabrication

To coat a thin and continuous metal shell on the magnetic core, our group have developed a sonochemically assisted hydroxylamine seeding growth method to synthesis MPPs (Fe_3O_4@Au). Firstly, magnetic Fe_3O_4 particles are synthesized through a modified solvothermal reaction.[67] An example transmission electron microscope (TEM) image of the synthesized Fe_3O_4 particles is shown in Fig. 2b. Secondly, the metal shell of the magnetic core is coated via three steps: a) hydrophilic Polyethyleneimine (PEI) is self-assembled on the surface of Fe_3O_4 particles as the linkers to form a Fe_3O_4@PEI microsphere under the sonication conditions (Fig. 2c). The thickness of PEI layer is controlled by adjusting the sonication time. b) Au seeds (small Au nanoparticles with the diameter of 3∼5nm) are grafted on Fe_3O_4@PEI to form monodispersed Fe_3O_4@PEI–AuNPs microspheres under the sonication conditions (Fig. 2d). These Au seeds act as the nucleation sites for the subsequent seed-mediated growth of the Au shell. c) $HAuCl_4$ is reduced by hydroxylamine hydrochloride and deposited on the Au seeds, affording a continuous and homogeneous Au shell around the Fe_3O_4 core (Fig. 2e). Finally, a PEI layer is modified around the MPPs to justify the surface property of the particles (Fig. 2f). The surface of MPPs can be modified by using other chemical or biological molecules, depending on the nature of the target to detect.

C. Typical characterization methods

The synthetic steps and all intermediates MPPs need to be characterized by a variety of techniques. Apart from standard scanning electron microscopy (SEM) and Transmission Electron Microscopy (TEM) techniques, X-ray diffraction (XRD), UV-visible absorption spectra, superconducting quantum interference device magnetometer (SQUID) characterization, and zeta potential measurements were also used.

The crystal structure and phase purity of the as-prepared products are usually characterized by XRD, as shown in Fig. 3a. The characteristic peaks of Fe_3O_4 are marked with "∗," and those of Au are marked with "#." Curve A represents a typical XRD pattern of the Fe_3O_4 particles.[80] After the absorption of the Au seeds, a new XRD peak (Curve B of Fig. 3a) can be observed at the diffraction peaks (2θ) of 38.2°, corresponding to the (111) crystalline plane of Au.[81] After a continuous Au shell forms outside the magnetic core, the diffraction peaks of Fe_3O_4 are no longer observed in Curve C of the Fe_3O_4@Au microspheres, which indicates the "complete coverage of the Fe_3O_4 core with Au shell."[78]

The size dispersity and the surface materials of the products are usually characterized by UV-visible absorption spectra, as shown in Fig. 3b. The broad peak band of Curve A illustrates the polydispersity of bare Fe_3O_4 microspheres, which can be attributed to the ferromagnetic behavior of the magnetic cores.[82] When the magnetic core is covered with Au seeds, the peak of the Fe_3O_4 shows a "red shift," indicating the growth of the particles. However, no additional peak was observed as the adhered Au seeds are too small to affect the plasmon behavior (Curve B). When the Fe_3O_4@Au microspheres are coated with a continuous Au shell, an obvious absorbance peak can be observed at 568 nm (Curve C), as a consequence of the surface plasmon coupling between the neighboring Au shells.[83]

The magnetic properties of products are usually assessed by SQUID, as shown in Fig. 3c. All of the curves nearly intersected with the origin, indicating that the remanence of the particles disappeared rapidly when the external magnetic confinement is removed. Thus, the synthesized particles are in a superparamagnetic state at the room temperature.[80] The saturation magnetization values tends to decrease slightly with the non-magnetic materials coating process. The magnetic separation of the MPPs is completed within 10s, even after the functionalization, as shown in the inset of Fig. 3c. The magnetic responsiveness provided by the MPPs are strong enough for target separation.

The surface charge properties of the products are characterized by the zeta potential measurements, as shown in Fig. 3d. After each step of PEI modification, the zeta potential of particles becomes strongly positive due to the cationic nature of the PEI polymer.

D. SERS application

To quantify the enhancement ability of the SERS substrate, the enhancement factor (EF) calculation and the detection limit determination are usually required.

EF is defined as a ratio of photons scattered by SERS substrate and normal substrate, and calculated according to the following formula.[84]

$$EF = \frac{I_{SERS}/N_{SERS}}{I_{NR}/N_{NR}} \tag{1}$$

Where I_{SERS} and I_{NR} are the Raman signal intensities measured on SERS-active substrate and non-SERS-active substrate (normal Raman), respectively; N_{SERS} and N_{NR} are the numbers of probe molecules contributing to the corresponding Raman signals I_{SERS} and I_{NR}. As an example, the EF of proposed MPPs substrate is calculated to be much higher than 10^7.

To determine the detection limit, controlled experiments are conducted using the MPPs as the SERS substrate. Herein, p-aminothiophenol (PATP) is used as a probe with concentrations ranging from 10^{-5} to 10^{-10} M. PATP detection limit of the MPPs substrate is 10^{-10} M judging from the vibration band at 1078 cm^{-1}, as shown in Fig. 4. The error bars in Fig. 4b indicate standard deviations from five measurements for each sample.

III. PLASMONIC CHARACTERISTICS

The Raman signal can be enhanced by 10^7 times or even more (enhancement factor) using the plasmonic particles as SERS substrate. It has been demonstrated that the

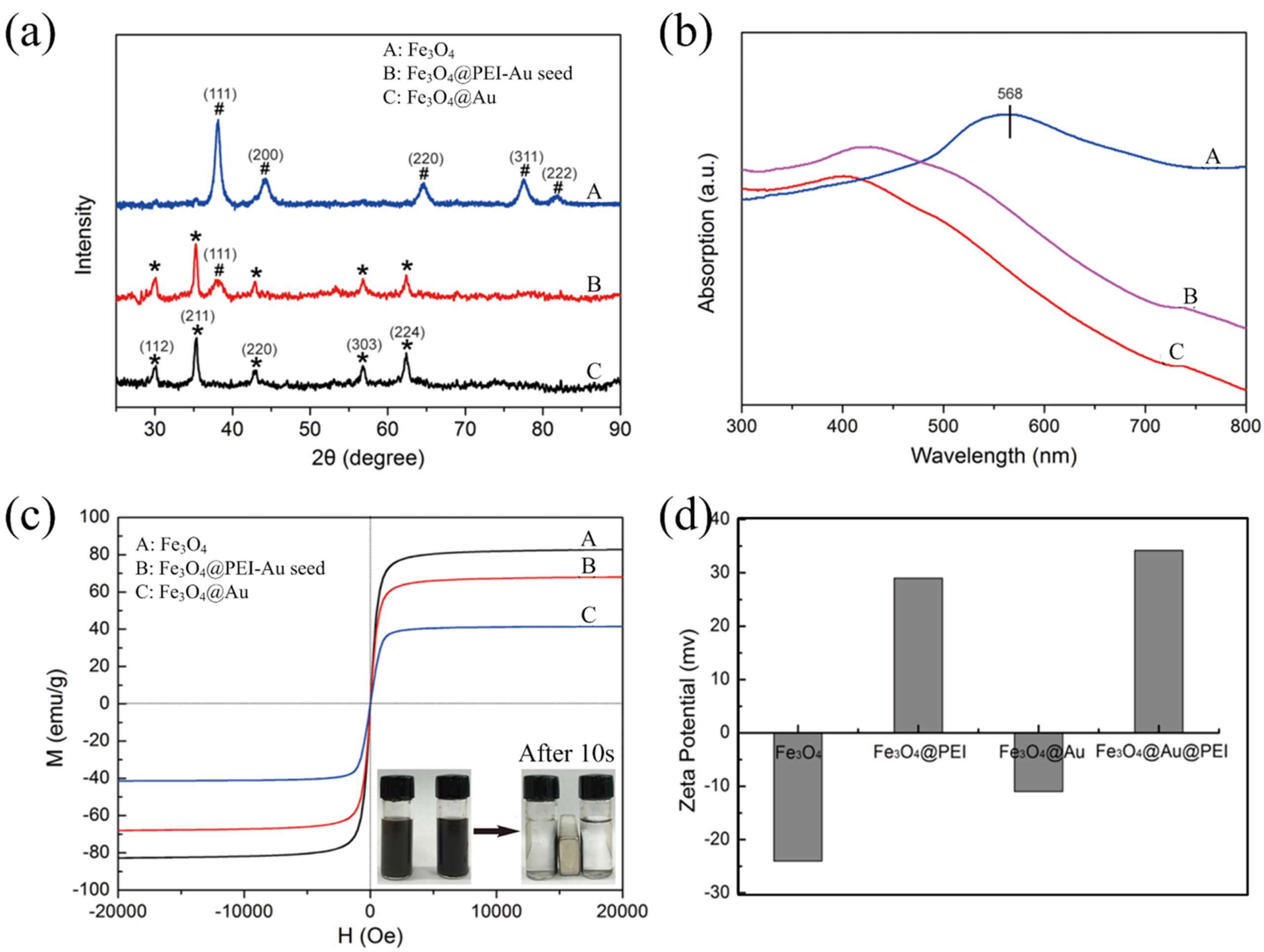

FIG. 3. Typical characterization methods for the MPPs. (a) XRD patterns, (b) UV-vis spectra, (c) magnetic hysteresis curves, and (d) statistical results of the zeta potential.

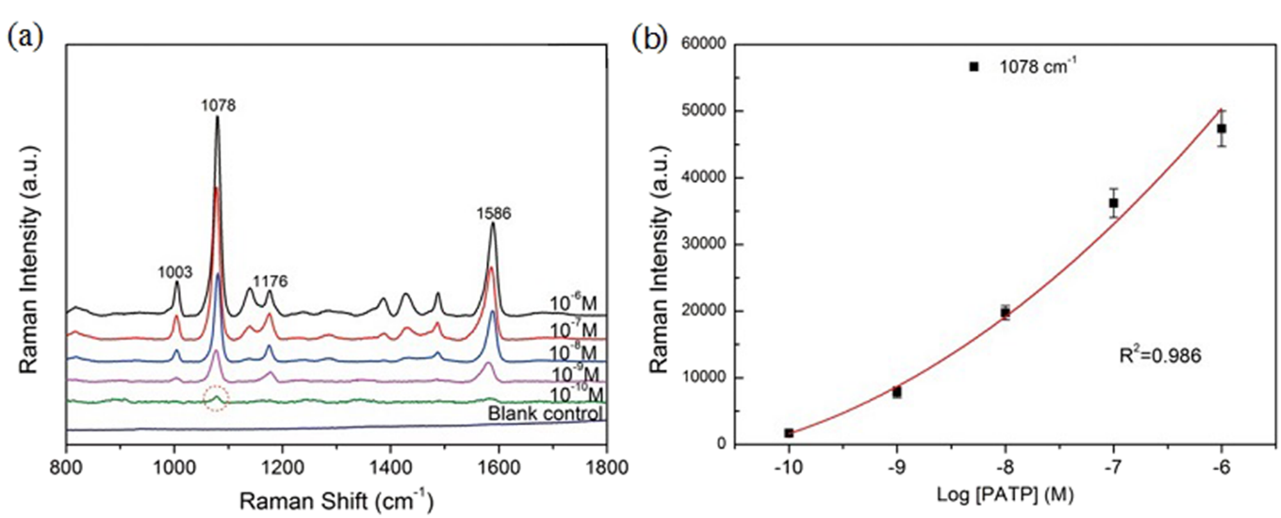

FIG. 4. (a) The SERS spectra of the PATP with various concentrations obtained from the MPPs and (b) their corresponding SERS intensities at the vibration band of 1078cm^{-1}.

dramatical enhancement was originated from both the physical mechanism and chemical mechanism. Since the chemical mechanism normally provides about 10~100 folds enhancement, the physical mechanism plays a predominant role in Raman signal enhancement, which is proportional to the fourth power of the EM field intensity. (Moskovits 1985) The area where the electromagnetic field concentrated or coupled are considered as the main factor that contributes to physical enhancement, which are usually called hotspots. The location and the strength of the hotspots can be investigated by solving the Maxwell equation. There are some sophisticated strategies as well as commercial available softwares for the numerical calculation, such as the FDTD, DDA, and etc. Recently, the FDTD method was the most popular one.

To investigate the plasmonic characteristics of the magnetic particles, FDTD method was employed for the visualization of the electromagnetic field on the surface of the particles. It is well known that single plasmatic particles provide limited EM field enhancement, thus can not form the hotspots. The hotspot usually located at the gap between neighborhood spherical NPs due to the electromagnetic field coupling. Three class of particles were studied, including the AgNPs, MPPs and magnetic particles. To simplify the calculation model, two NPs system were employed herein. To make the hotspot locate at the center of the two NPs, not around the junction, the NPs was fixed to be 1nm apart.

The EM field coupled at the gap between the particles as shown in Fig. 5(a~c). The EM field enhancement of three particles at the wavelength ranging from 300nm~900nm was shown in Fig. 5d. The Ag NPs are typical plasmatic particles, which can provide sufficient EM field enhancement at the gap. The MPPs can provide similar EM field enhancement. The magnetic core gave limited effection to the plasmatic characteristic of the particle. The surface plasma was mainly provided by the Ag shell. However, the peak of the enhancement curve was blue shift due to the addition of the magnetic core. The bare magnetic particles provide little EM field enhancement because no surface plasma was excited by the laser. To sum up, the bare magnetic particles can not provide surface plasma, while the addition of magnetic core will not affect of the plasmatic characteristics of the noble metallic particles.

IV. LABEL-FREE BACTERIA DETECTION

A. Sensing principle

As mentioned, label-free method detects the intrinsic SERS fingerprint of bacteria without using a label, making the process usually fast and relatively simple. The characteristic spectra of the bacteria is largely determined by the components of their cell wall, such as polysaccharides, amino acids, nucleic acid, lipids, carbohydrates, and proteins.[27–31] The tentative assignments of the spectra peaks have been summarised in many previously published literatures.[85–87] Label-free detection method can not only distinguish species of bacteria,[88,89] but can also identify whether the bacteria is live or dead.[90,91] Label-free bacteria sensing presents the new frontier of cell-based assays.[85] Two main challenges still hinder the wide applications of the label-free method: the sensitivity improvement and the bacteria enrichment. To date, the spectra intensity of the cell wall components is very weak. In addition, the components cannot be positioned right at the hotspots of the SERS substrate, which will seriously affect the sensitivity of the sensing method. Thus, the performance of the SERS substrate is a key factor for label-free bacteria detection method. Moreover, enriching the bacteria and avoiding the interference from the impurities is essential for the real sample testing. Mosier-Boss's group,[92,93] and Evelin Witkowska's group[94] have enriched the bacteria cell on/around the SERS substrate by a filtering process. However such strategy can introduce some interference spectra due to the presence of big molecules in the sample. Yu's group[95] generates enriched bacteria by using a multiplexing self-referencing SERS microfluidic. Despite promising, long

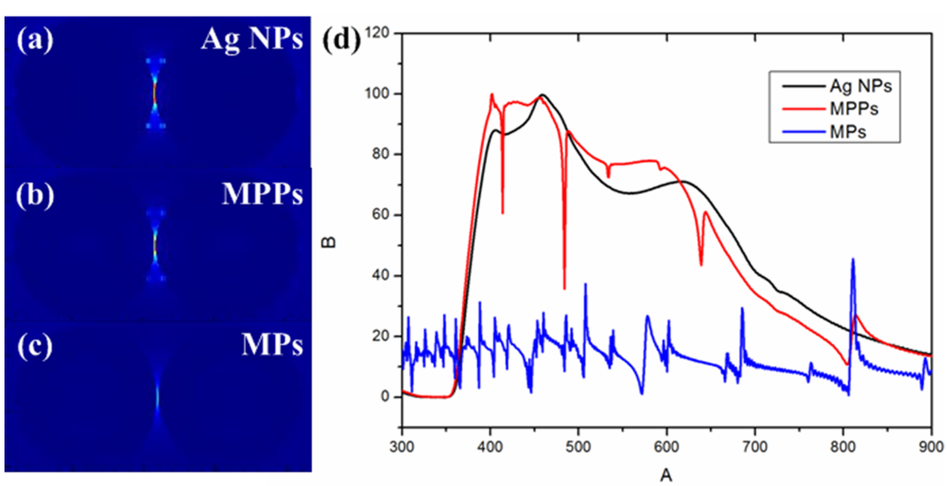

FIG. 5. Plasmonic characteristics of (a) AgNPs, (b) MPPs, and (c)MPs. (d) The EM field enhancement curve at the wavelength ranging from 300nm to 900nm.

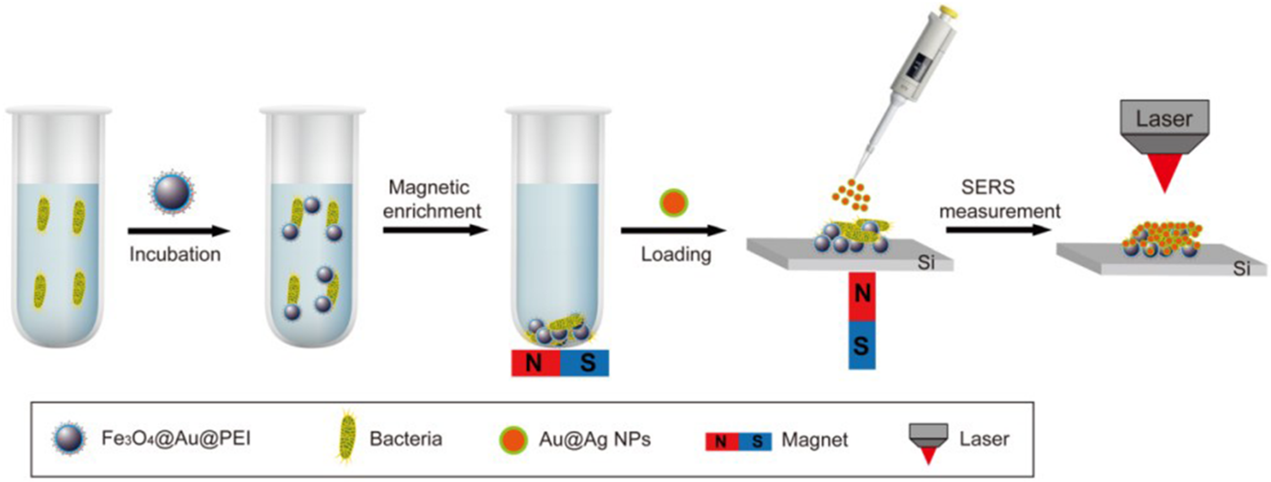

FIG. 6. Schematic diagram of the CEE procedure for the rapid SERS detection of the bacteria.

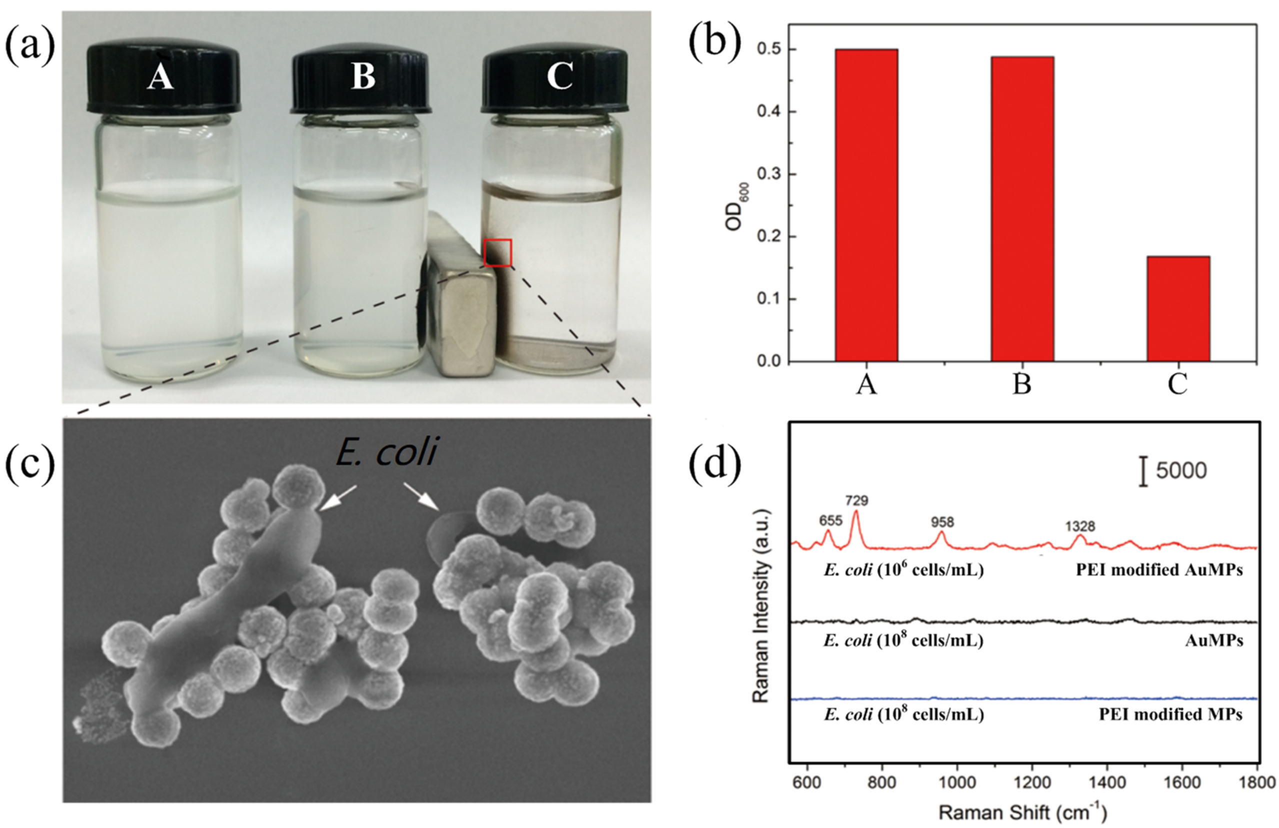

FIG. 7. Efficiency characterization of MPPs to capture E. coli from the solution. (a) Photo images of (A) E. coli solution, (B) solution after magnetic capture by bare MPPs, and (C) solution after magnetic capture by PEI modified MPPs. (b) The corresponding bacteria concentration of the supernatant by testing OD_{600}. (c) The TEM image of the enriched bacterial aggregation. (d) The SERS spectral of E. coli captured by various particles under different conditions.

times are needed (about 17 hours) to process samples (1 mL, at a flow rate of 1 μL/min).

Given these challenges, we have brought out a capture–enrichment–enhancement (CEE) method for the rapid and sensitive bacteria detection. A kind of novel MPPs (Fe_3O_4@Au microspheres) is synthesized and used as SERS substrate. The MPPs are positively charged by the presence of an amino-functionalised polymer. Then, MPPs are dropped into the bacteria solution and incubated for 5 min. During this process, the negatively charged bacteria are rapidly captured and separated by the positively charged MPPs under an external magnetic confinement, resulting in the enrichment of the bacteria. The separated composites are consequently dropped on a clean Si substrate and followed by the addition of concentrated Au@Ag NPs to further improve enhancement. The Au@Ag NPs can cover the blank surface of bacteria, and produce more hotspots. The schematic of CEE procedure for the rapid SERS detection of bacterial pathogens is shown in Fig. 6.

B. Bacteria capturing and enrichment

To capture and enrich the bacteria, the amino-groups of the PEI are firstly protonated to afford a positive charge on MPPs surface. This causes a strong electrostatic interaction between the MPPS surface and negatively charged bacterial walls, thus capturing the bacteria in the solution. To evaluate the bacterial capture ability of the MPPs, Escherichia coli. (E. coli.) is used as an example and its optical density(OD) at the wavelength of 600nm (OD_{600}) is measured. The concentration of bacteria is adjusted to a OD_{600} of 0.5 at first as shown in Photo A in Fig. 7a. The MPPs with and without PEI-functionalization are added into the *E. coli* solution and incubated for 5 min, respectively. After the magnetic aggregation, the supernatant solution added with bare MPPs (i.e., Photo B in Fig. 7a) appears nearly the same as that of original *E. coli* solution (i.e., photo A in Fig. 7a), while the supernatant solution added with PEI modified MPPs becomes nearly transparent (i.e., photo C in Fig. 7a). The OD_{600} testing confirms the contribution of PEI layer in bacteria

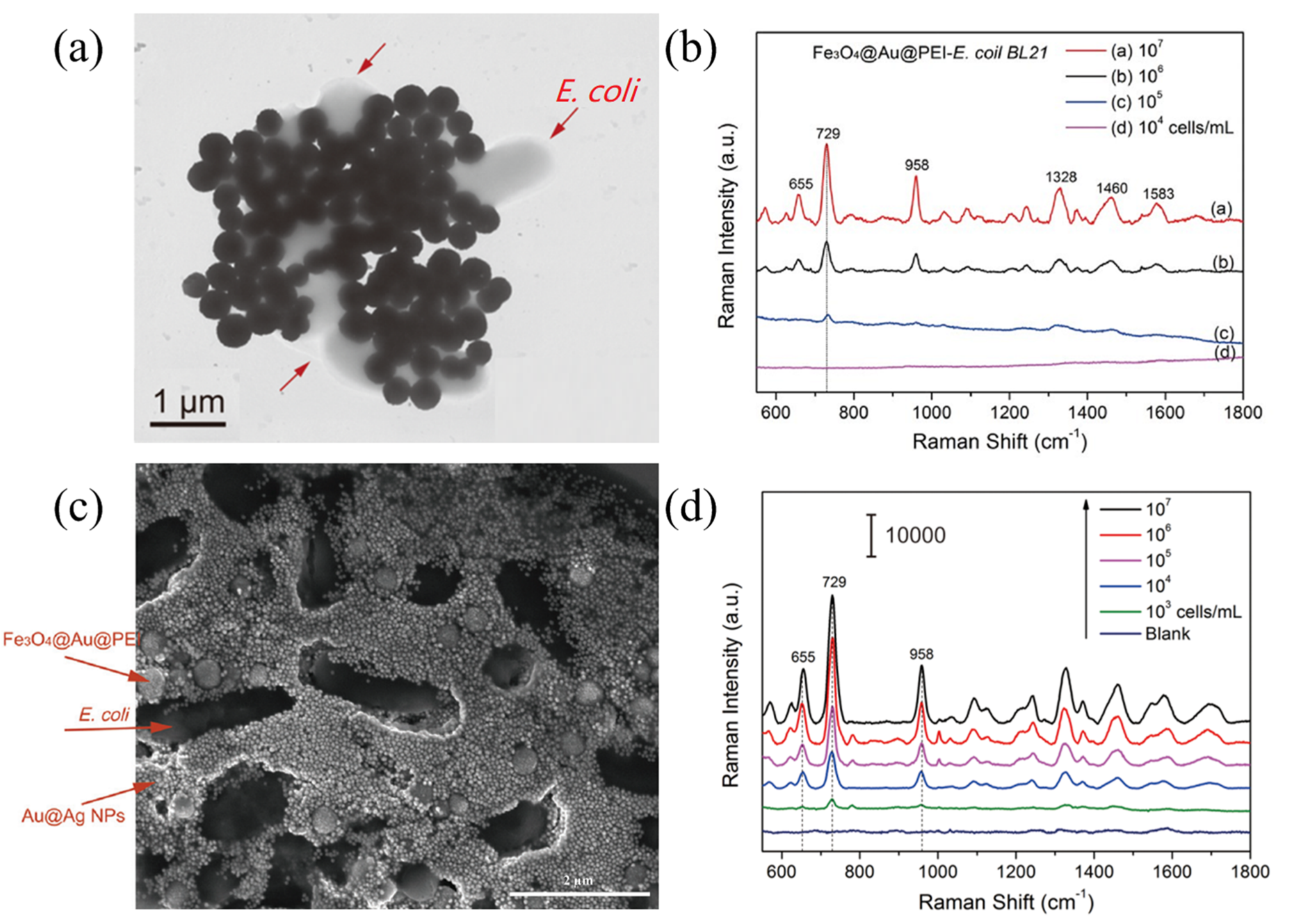

FIG. 8. (a, c) TEM and SEM images of the MPPs-bacterial aggregation without and with the Au@Ag NPs addition, respectively. (b, d) SERS spectra of E. coli BL21 with different concentrations obtained via the MPPs and CEE method, respectively.

capturing. The capture efficiency (CE) of the PEI-functionalized MPPs is calculated to be 66.2% following the formula CE (%) = 100(α - β)/α, where α and β represent the OD_{600} values before and after magnetic separation.[96] HOW?? (Fig. 7b). Fig. 7c shows the TEM image of MPPs-bacteria complex. The MPPs are conjugated tightly outside E. coli., facilitating Raman signal enhancement as illustrated in Fig. 7d. The major vibrational modes of *E. coli* can be observed at the concentration of 10^6 cells/mL, as it is captured by the MPPs microspheres, while no characteristic vibrational bands are observed even at the bacterial concentration of 10^8 cells/mL mixed with Fe_3O_4@Au and Fe_3O_4@PEI microspheres. Capturing the bacterial cells is based on the electrostatic interaction between the positively charged MPPs and the negatively charged bacteria walls. Thus, the amine groups modified on the MPPs are potentially nonselective ligands to various types of bacteria because the cell walls of bacteria are generally negatively charged.[97]

C. Sensitivity improvement

To determine the sensitivity of prepared SERS substrate, SERS spectra of E. coli are obtained at different concentrations ranging from 1×10^7 cells/mL to 1×10^2 cells/mL. The detection limit of MPPs is about 1×10^5 cells/mL, insufficient for bacteria sensing. A scattered distribution of AuNPs around the bacteria can be observed in Fig. (8)(a, b). To improve the sensitivity, Au@Ag core-shell NPs are used as reinforced nanoparticles to further cover the bacteria surface, providing additional hotspots as shown in Fig. 8c. The bacteria SERS signals are synergistically enhanced by the MPPs and Au@Ag NPs, especially at the conjunctions. The intensity of the SERS signals obviously increase by about 2 orders of magnitude, as shown

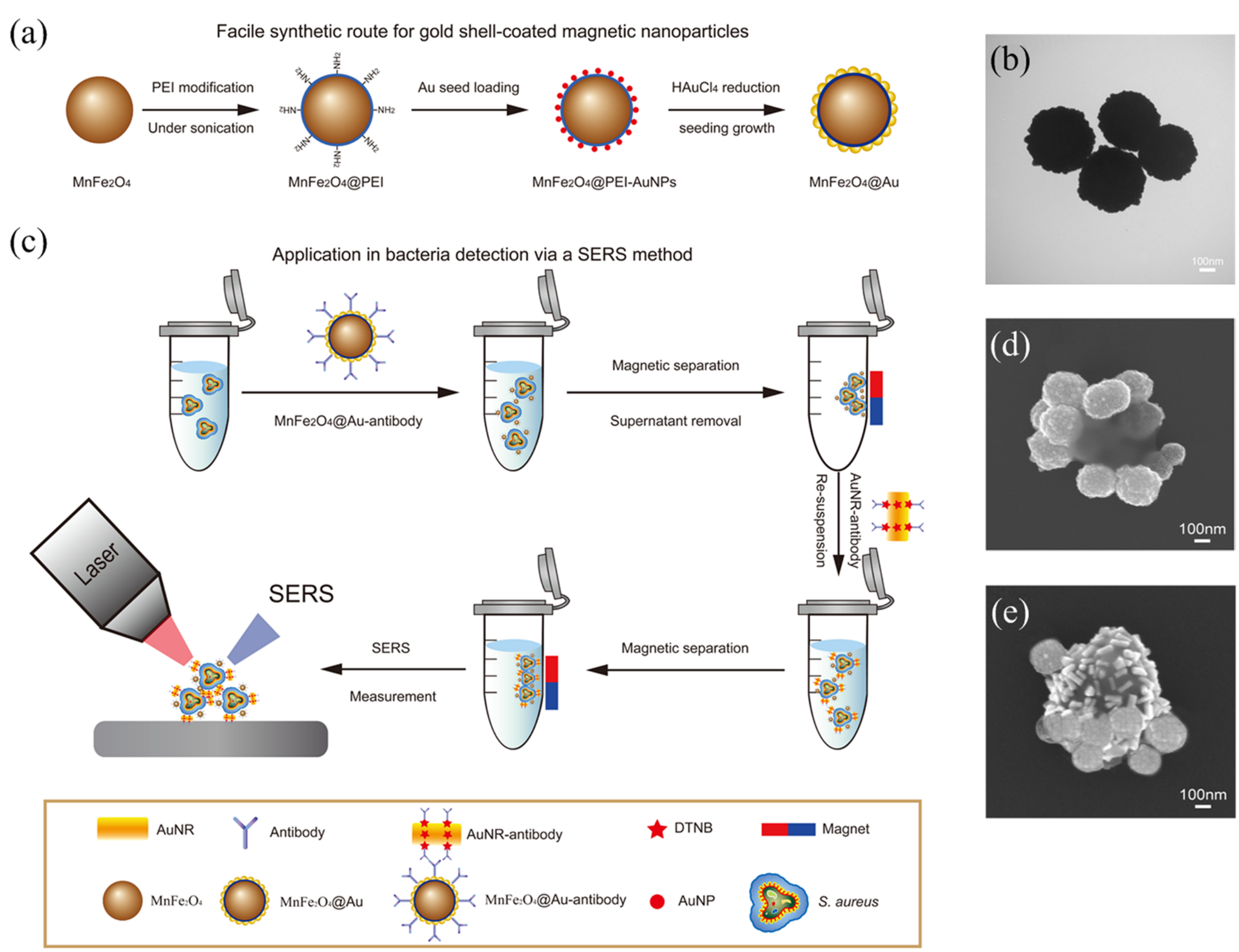

FIG. 9. Synthetic route of the SERS-based immuno-sensing method and TEM images of each step. (a) Synthetic route and (b) TEM image of gold shell-coated magnetic nanoparticles, (c) schematic illustration of the operating procedures for bacteria detection via a SERS method, TEM images of (d) S. aureus binding to antibody-conjugated MPPs and (e) MPPs-bacteria-SERS-tag sandwich architecture.

in Fig. 8d. The detection limit is about 10^3 cells/mL for both Gram-positive bacterium E. coli and Gram-positive bacterium S. aureus, which is comparable to that of the PCR method. The whole process, from the bacteria capture to SERS signal measurements, can be completed within 10 minutes.

The selectivity of this label-free sensing strategy is based on the instinct Raman fingerprints of the bacterial cell. To easily distinguish the spectra of the bacterial, principle component analysis (PCA) method was usually applied.[95] PCA method can reduce the dimensionality of multivariate spectral data and group the similar spectral data for classification. Generally speaking, the more samples PCA method include, the more accurate should the distinguish process be.

V. LABEL-BASED BACTERIA DETECTION

Label-based bacteria detection is an extrinsic mode method, which reports the target indirectly by collecting and analyzing signals of the so-called SERS-tag. SERS-tag is a kind of novel nanoprobe, which combines metallic NPs and organic Raman reporter molecules to give rise to strong and specified Raman signals.[98–100] The typical sandwich structure is usually constructed with the aid of specific ligands such as antibodies and aptamers. Thus, the selectivity of the assay is based on the specific recognition of the ligands. The sandwich structure contains a MPPs as the SERS substrate, a captured bacteria as the target and a SERS-tag as the reporter. Hotspots are created at the junctions between MPPs and SERS-tag at the appearance of target bacteria.

A. Immuno-sensing

The SERS-based immuno-assay for the bacteria is based on the construction of sandwich complex by the specific antigen-antibody conjugations, as illustrated in Fig. 9. Herein, Au coated MFe_2O_4 particles are utilized as the MPPs, the Staphylococcus aureus (S. aureus) are employed as the target, and the 5,5'-dithiobis-(2-nitrobenzoic acid) (DTNB) marked nanorod is used as the SERS-tag. Preparation of the proposed MPPs is similar to that introduced above, as shown in Fig. 2a. The prepared MPPs are modified with selected antibody and incubated in the S. aureus solution for the specific bacteria capture. The particles containing captured S. Aureus. are then separated by an external magnet, a more effective and simpler method compared to traditionally used centrifugation. The uncaptured bacteria that remains in the supernatant are consequently removed. The second-antibody modified SERS-tag is dropped into the suspended solution to construct the sandwich structure. The bacteria have respective conjugation sites for the antibody and second-antibody, as shown in Fig. 9b. Finally, the sandwich complex is separated and placed on a supporting silicon slice for SERS measurements.

By using an antibody as both recognizer and linker, selective detection of S. *aureus* is achieved with a detection limit down to 10 cells/mL. To quantify the dose-response of the proposed method, a calibration curve between the SERS intensity at the vibration band at 1331 cm^{-1} and the logarithm of S. *aureus* bacteria concentrations (10^1–10^5 cells/mL) has been plot and is shown in Fig. 10b. A good linear relationship was obtained with a correlation coefficient of 0.9789. The error bars represent the standard deviations from five measurements for each sample.

B. Aptamer recognition sensing

Aptamers are single–stranded DNA or RNA molecules that can bind to target bacteria with high affinity and specificity. Similar to antibodies, aptamers also serve both as the recognizer and linker in the sandwich structure construction.

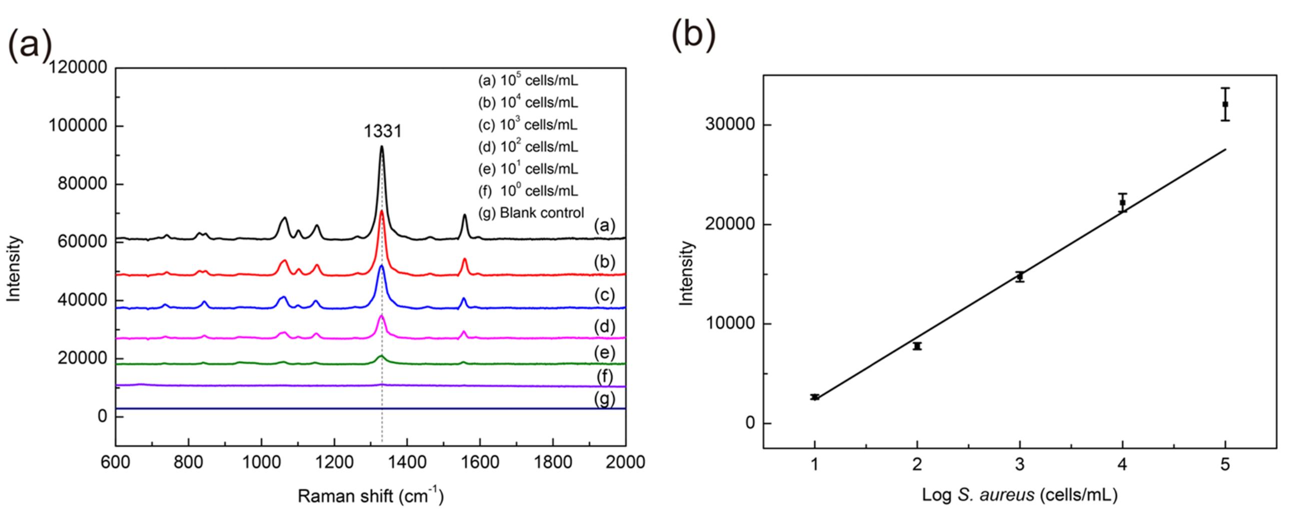

FIG. 10. (a) SERS spectra taken from the immuno-sensing platform with various concentrations of *S. aureus* (10^5, 10^4, 10^3, 10^2, 10^1, and 10^0 cells/mL) and blank control. (b) Calibration curve for *S. aureus* at a concentration range of $10^1 \sim 10^5$ cells/mL.

However, they have advantages over the antibodies. Firstly, screening process is both time-saving and cost-effective, known as the systematic evolution of ligands by exponential enrichment (SELEX). It is an in vitro selection process which usually takes 2 to 3 months (the quickest being 2 weeks) in contrast to at least 3 to 6 months required by monoclonal antibody preparation. Secondly, aptamers have better chemical stability than antibodies. Aptamers possess a certain degree of thermal annealing features, and can maintain chemically stable over a wide pH range from 2 to 12, whereas antibodies are easily denatured due to their protein nature. Thirdly, aptamers can be flexibly modified with functional groups because it can be synthesized with a simple and cost-effective chemical method. As a better replacement of antibodies, aptamers have been widely used in bacteria detection, and some even in cancer cells detection.[101–106]

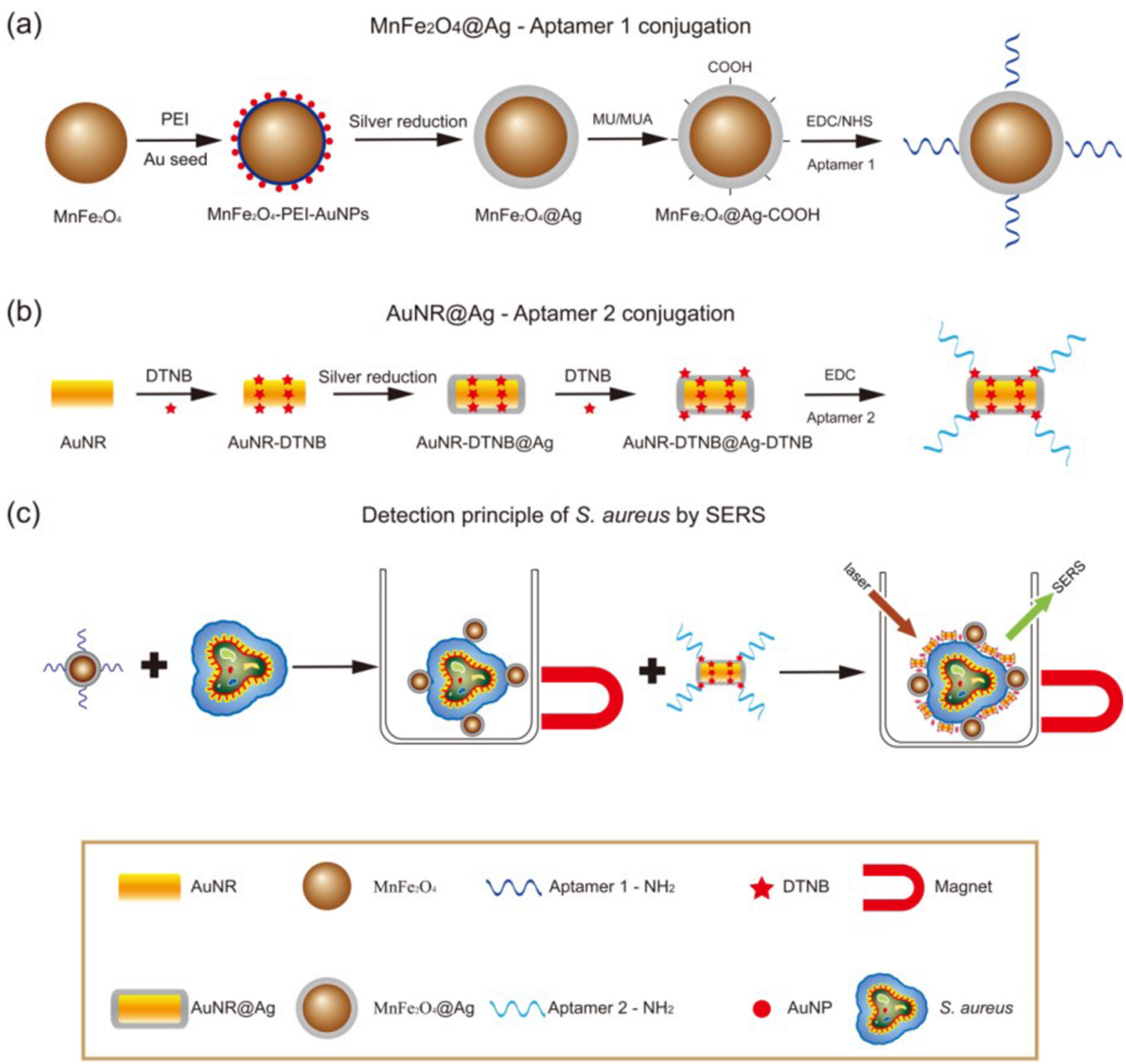

FIG. 11. Schematic illustration of aptamer recognition *S. aureus* detection using the SERS method. Synthesis and functionalization of (a) the MPPs and (b) the SERS-tag. (c) the operating principle for *S. aureus* detection.

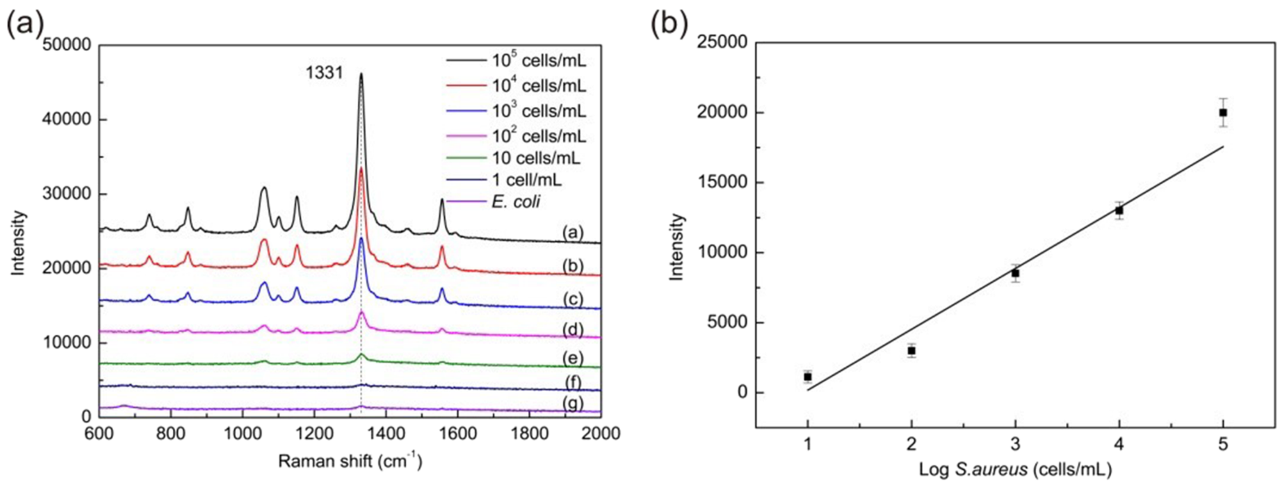

FIG. 12. (a) SERS spectra taken from the aptamer recognition sensing platform with various concentrations of *S. aureus* (10^5, 10^4, 10^3, 10^2, 10^1, and 10^0 cells/mL) and *E. coli* (10^5 cells/mL). (b) Calibration curve for *S. aureus* at a concentration range of $10^1 \sim 10^5$ cells/mL considering the SERS intensity at 1331 cm^{-1}.

Herein, Ag coated $MnFe_2O_4$ ($MnFe_2O_4$@Ag) particles are used as the MPPs, synthesized through the "seed–mediated growth" method and modified with Aptamer-1 as shown in Fig. 11a. A novel SERS-tag, with DTNB–labeled inside–and–outside plasmonic NPs, is prepared and modified with aptamers, as shown in Fig. 11b. The sensing principle is similar to that of immuno-assay, but forms an aptamer-target-aptamer sandwich complex, as shown in Fig. 11c.

The S. aureus with various concentrations ranging from 1 to 10^5 cells/mL are tested with the aptamer recognition method. The SERS spectra of Raman reporter molecule (DTNB) are shown in Fig. 12a. The signal intensities attenuate concomitantly with the decrease of S. Aureus concentration. The detection limit is 10 cell/mL. To further explore the dose-response of S. Aureus, a calibration curve between Raman intensities and logarithm of S. aureus bacteria concentrations

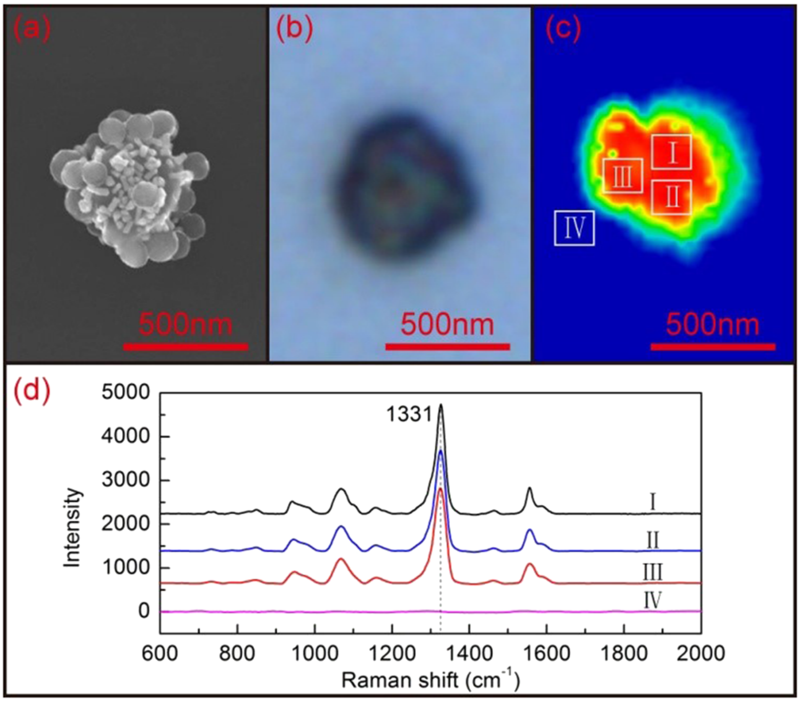

FIG. 13. Single–cell detection of S. aureus by SERS mapping method. The corresponding (a) SEM image, (b) optical image, and (c) SERS intensity map of aptamer recognition sandwich architecture. (d) Average SERS spectrum obtained from the different regions of (c).

TABLE I. The characteristics of recently reported methods for bacteria detection.

Target	Detection method	Dynamic range (cfu/mL)	Detection limit (cfu/mL)	Reference
S. aureus	Colorimetric	$10\text{-}10^6$	9	Yuan et al. 2014[102]
S. aureus	Colorimetric	$1.5\times10^3\text{-}1.5\times10^5$	1.5×10^3	Sung et al. 2013[107]
E. coli	Two-Photon Rayleigh Scattering	50-2100	50	Singh et al. 2009[108]
S. aureus	Anisometric	$4.4\times10^5\text{-}1.8\times10^7$	1.7×10^5	Escamilla-Gómez et al. 2008[109]
S. aureus	Anisometric	$10\text{-}10^8$	10	Majumdar et al. 2013[110]
S. aureus	Potentiometric	$10^3\text{-}10^8$	8×10^2	Zelada-Guillén et al. 2012[111]
E. coli	SERS	$3.5\times10^2\text{-}3.5\times10^7$	35	Tamer et al. 2012[112]
E. coli	SERS	$10^3\text{-}10^7$	10^3	Wang et al. 2016[113]
S. aureus	SERS	$10^3\text{-}10^7$	10^3	Wang et al. 2016[113]
S. aureus	SERS	$10\text{-}10^5$	10	Wang et al. 2015[114]
S. aureus	SERS	$10\text{-}10^5$	10	Wang et al. 2016[115]

is plotted with regarding the vibration band at 1331 cm^{-1}, as shown in Fig. 12b. The calibration line exhibited a good linearity with a correlation coefficient of 0.9558 under the bacteria concentrations ranging from 10 to 10^5 cells/mL.

With the aid of a newly-developed SERS mapping technique, single cell detection of bacteria becomes feasible following the proposed sensing method as shown in Fig. 13. The SEM and optical images of the final MPPs-target-SERS-tag sandwich complex are shown in Fig. 13 (a) and (b), respectively. The SERS mapping image is shown in Fig. 13c. The map color corresponds to the SERS intensity at the vibration band of at 1331 cm^{-1}. The shape of the mapping image generally depends on the distribution of the SERS-tag that bound on the surface of the bacteria. The SERS spectra acquired from different spots of the sandwich complex are plotted in Fig. 13d. The ability of single cell detection demonstrates the excellent sensitivity of the aptamer recognition sensing method.

Comparing with other recently reported methods, the SERS technique performs better or equivalent well for the bacteria detection, as demonstrated in Table I,[102,107–115] and offers advantages of shorter time and easier operation process. The label-based sensing strategy possesses a better sensitivity than the label-free one, even down to the single cell level, by detecting the spectra of the SERS-tag instead of the instinct spectra of the bacteria. The molecules with good SERS activity are usually selected as the report molecules and immobilized on the SERS-tag. These report molecules are located right at the hotspots area, i.e. at the gap between the MPP and the SERS-tag in the SERS measurements. Thus, the SERS-tag serves as an effective amplifier and transducer in the sensing system, leading to improved sensitivity by two orders of magnitude. Compared with the label-based method, label-free one is more robust and simpler; albeit lower, the sensitivity of the label-free method is often acceptable in many cases. There advantages make the label-free method a better candidate for rapid and on-site bacteria filtration. In addition, by detecting the intrinsic spectra of the bacteria, the label-free method can be utilized to characterize the physiological state of the bacteria.

VI. CONCLUDING REMARKS

The good physical properties, cost-effective synthesis, ease of control, and the flexible functionizability make the MPPs a versatile platform for the pathogen bacteria cell detection. The inner magnetic core provides MPP with good magnetic responsivity. And the outer noble metal shell provided with excellent plasmonic activity. It is fundamental to cover the magnetic core with a thin and continuous noble metal, as it can give rise to good SERS performance without affecting the magnetic prosperity significantly. By using an external magnet, MPPs can be easily manipulated to facilitate the target separation and enrichment, performing favorably over the commonly used centrifugation process which may lead to unwanted particle aggregation. The adaptable functionalization confers to MPPs an appropriate affinity and selectivity towards target analyte. Taking advantage of the particular chemistry or biology groups at the surface of MPPs, the capture efficiency can be improved and the proposed SERS platform can be expanded over a broad range of biological conditions.

The combination of advanced MPPs and the promising SERS technique has paved the way for sensitive, selective, rapid and cost-effective bacteria sensing. Despite these remarkable developments, however, challenges remain. Systematical studies are required in the immediate future to improve the reproducibility of the detection method, especially for the quantitative analysis, as the SERS signal is highly sensitive to the size, shape and distribution of the particles. In addition, the whole-organism fingerprinting database should be built for the competent bacteria sensing. The database is of particularly importance for the label-free detection. Moreover, optimization of parameters for the sensing systems is still required to meet the demands of clinical diagnostics for the future development of personalized medicine. The fundamental advantages of MPPs have generated a dramatic increase in their use in the bacterial sensing, which will continue to rapidly evolve, along with advances in other fields such as microfluidics, molecular biology, analytical chemistry, and self-assembly techniques. This will open many great opportunities for coordinated international studies and continue to revolutionize the field of diagnostics for years to come.

ACKNOWLEDGMENTS

This work was funded by National Natural Science Foundation of China under Grant No. 51605486 and No. 51475468. Dr Marco M. Meloni is supported by the British Heart Foundation (BHF, FS/15/17/31411).

REFERENCES

[1]A. Dong, S. Lan, J. Huang, T. Wang, T. Zhao, L. Xiao, W. Wang, X. Zheng, F. Liu, G. Gao, and Y. Chen, "Modifying Fe_3O_4-functionalized nanoparticles with N-halamine and their magnetic/antibacterial properties," ACS Applied Materials & Interfaces **3**(11), 4228–4235 (2011).

[2]H. Zhou, D. Yang, N. P. Ivleva, N. E. Mircescu, R. Niessner, and C. Haisch, "SERS detection of bacteria in water by in situ coating with Ag nanoparticles," Anal Chem **86**(3), 1525–1533 (2014).

[3]A. Walter, A. Marz, W. Schumacher, P. Rosch, and J. Popp, "Towards a fast, high specific and reliable discrimination of bacteria on strain level by means of SERS in a microfluidic device," Lab Chip **11**(6), 1013–1021 (2011).

[4]S. Buchanan, E. C. Le Ru, and P. G. Etchegoin, "Plasmon-dispersion corrections and constraints for surface selection rules of single molecule SERS spectra," Phys Chem Chem Phys **11**(34), 7406–7411 (2009).

[5]D. van Lierop, K. Faulds, and D. Graham, "Separation free DNA detection using surface enhanced Raman scattering," Analytical Chemistry **83**(15), 5817–5821 (2011).

[6]D. Yang, H. Zhou, C. Haisch, R. Niessner, and Y. Ying, "Reproducible E. coli detection based on label-free SERS and mapping," Talanta **146**, 457–463 (2016).

[7]H. Zhou, D. Yang, N. P. Ivleva, N. E. Mircescu, S. Schubert, R. Niessner, A. Wieser, and C. Haisch, "Label-free in situ discrimination of live and dead bacteria by surface-enhanced Raman scattering," Analytical Chemistry **87**(13), 6553–6561 (2015).

[8]S. K. Srivastava, H. B. Hamo, A. Kushmaro, R. S. Marks, C. Gruner, B. Rauschenbach, and I. Abdulhalim, "Highly sensitive and specific detection of E. coli by a SERS nanobiosensor chip utilizing metallic nanosculptured thin films," The Analyst **140**(9), 3201–3209 (2015).

[9]X. Lu, D. R. Samuelson, Y. Xu, H. Zhang, S. Wang, B. A. Rasco, J. Xu, and M. E. Konkel, "Detecting and tracking nosocomial methicillin-resistant Staphylococcus aureus using a microfluidic SERS biosensor," Analytical Chemistry **85**(4), 2320–2327 (2013).

[10]C. Wang, R. Xiao, P. Dong, X. Wu, Z. Rong, L. Xin, J. Tang, and S. Wang, "Ultra-sensitive, high-throughput detection of infectious diarrheal diseases by portable chemiluminescence imaging," Biosensors and Bioelectronics **57**(0), 36–40 (2014).

[11]J. F. Li, Y. F. Huang, Y. Ding, Z. L. Yang, S. B. Li, X. S. Zhou, F. R. Fan, W. Zhang, Z. Y. Zhou, D. Y. Wu, B. Ren, Z. L. Wang, and Z. Q. Tian, "Shell-isolated nanoparticle-enhanced Raman spectroscopy," Nature **464**(7287), 392–395 (2010).

[12]E. J. Titus, M. L. Weber, S. M. Stranahan, and K. A. Willets, "Super-resolution SERS imaging beyond the single-molecule limit: An isotope-edited approach," Nano Lett **12**(10), 5103–5110 (2012).

[13]C. Wang, X. Wu, P. Dong, J. Chen, and R. Xiao, "Hotspots engineering by grafting Au@Ag core-shell nanoparticles on the Au film over slightly etched nanoparticles substrate for on-site paraquat sensing," Biosensors and Bioelectronics **86**, 944–950 (2016).

[14]R. Gao, N. Choi, S. I. Chang, S. H. Kang, J. M. Song, S. I. Cho, D. W. Lim, and J. Choo, "Highly sensitive trace analysis of paraquat using a surface-enhanced Raman scattering microdroplet sensor," Anal Chim Acta **681**(1-2), 87–91 (2010).

[15]A. Kim, S. J. Barcelo, R. S. Williams, and Z. Li, "Melamine sensing in milk products by using surface enhanced Raman scattering," Anal Chem **84**(21), 9303–9309 (2012).

[16]T. Kang, S. M. Yoo, M. Kang, H. Lee, H. Kim, S. Y. Lee, and B. Kim, "Single-step multiplex detection of toxic metal ions by Au nanowires-on-chip sensor using reporter elimination," Lab Chip **12**(17), 3077–3081 (2012).

[17]Y. C. Cao, R. Jin, and C. A. Mirkin, "Nanoparticles with Raman spectroscopic fingerprints for DNA and RNA detection," Science **297**(5586), 1536–1540 (2002).

[18]T. Kang, S. M. Yoo, I. Yoon, S. Y. Lee, and B. Kim, "Patterned multiplex pathogen DNA detection by Au particle-on-wire SERS sensor," Nano Letters **10**(4), 1189–1193 (2010).

[19]H. Zhang, M. H. Harpster, H. J. Park, P. A. Johnson, and W. C. Wilson, "Surface-enhanced Raman scattering detection of DNA derived from the West Nile virus genome using magnetic capture of Raman-active gold nanoparticles," Analytical Chemistry **83**(1), 254–260 (2010).

[20]H. Zhou, D. Yang, N. P. Ivleva, N. E. Mircescu, R. Niessner, and C. Haisch, "SERS detection of bacteria in water by in situ coating with Ag nanoparticles," Analytical Chemistry **86**(3), 1525–1533 (2014).

[21]S. S. Dasary, A. K. Singh, D. Senapati, H. Yu, and P. C. Ray, "Gold nanoparticle based label-free SERS probe for ultrasensitive and selective detection of trinitrotoluene," J Am Chem Soc **131**(38), 13806–13812 (2009).

[22]L. Zhang, C. Jiang, and Z. Zhang, "Graphene oxide embedded sandwich nanostructures for enhanced Raman readout and their applications in pesticide monitoring," Nanoscale **5**(9), 3773–3779 (2013).

[23]A. P. Craig, A. S. Franca, and J. Irudayaraj, "Surface-enhanced Raman spectroscopy applied to food safety," Annu Rev Food Sci Technol **4**, 369–380 (2013).

[24]W. Chaoguang, X. Rui, W. Xuezhong, D. Peitao, R. Zhen, C. Jian, and W. Shengqi, "Ultrasensitive hybrid SERS substrate for rapid detection of trace chemicals," Laser Phys **24**(4), 045807 (2014).

[25]Y. Wang, S. Ravindranath, and J. Irudayaraj, "Separation and detection of multiple pathogens in a food matrix by magnetic SERS nanoprobes," Analytical and Bioanalytical Chemistry **399**(3), 1271–1278 (2010).

[26]X. Wu, C. Xu, R. A. Tripp, Y. W. Huang, and Y. Zhao, "Detection and differentiation of foodborne pathogenic bacteria in mung bean sprouts using field deployable label-free SERS devices," The Analyst **138**(10), 3005–3012 (2013).

[27]R. M. Jarvis and R. Goodacre, "Characterisation and identification of bacteria using SERS," Chemical Society Reviews **37**(5), 931–936 (2008).

[28]C. C. Lin, Y. M. Yang, P. H. Liao, D. W. Chen, H. P. Lin, and H. C. Chang, "A filter-like AuNPs@MS SERS substrate for Staphylococcus aureus detection," Biosensors & Bioelectronics **53**, 519–527 (2014).

[29]R. M. Jarvis, A. Brooker, and R. Goodacre, "Surface-enhanced Raman scattering for the rapid discrimination of bacteria," Faraday Discuss **132**, 281–292 (2006).

[30]C. Fan, Z. Hu, A. Mustapha, and M. Lin, "Rapid detection of food- and waterborne bacteria using surface-enhanced Raman spectroscopy coupled with silver nanosubstrates," Appl Microbiol Biotechnol **92**(5), 1053–1061 (2011).

[31]M. Kahraman, K. Keseroğlu, and M. Çulha, "On sample preparation for surface-enhanced Raman scattering (SERS) of bacteria and the source of spectral features of the spectra," Appl Spectrosc **65**(5), 500–506 (2011).

[32]X. Wu, Y. W. Huang, B. Park, R. A. Tripp, and Y. Zhao, "Differentiation and classification of bacteria using vancomycin functionalized silver nanorods array based surface-enhanced Raman spectroscopy and chemometric analysis," Talanta **139**, 96–103 (2015).

[33]S. C. Luo, K. Sivashanmugan, J. D. Liao, C. K. Yao, and H. C. Peng, "Nanofabricated SERS-active substrates for single-molecule to virus detection in vitro: A review," Biosens Bioelectron **61**, 232–240 (2014).

[34]R. Gordon, D. Sinton, K. L. Kavanagh, and A. G. Brolo, "A new generation of sensors based on extraordinary optical transmission," Acc Chem Res **41**(8), 1049–1057 (2008).

[35]Q. Yu and G. Golden, "Probing the protein orientation on charged self-assembled monolayers on gold nanohole arrays by SERS," Langmuir **23**(17), 8659–8662 (2007).

[36]C. M. Kolodziej and H. D. Maynard, "Electron-beam lithography for patterning biomolecules at the micron and nanometer scale," Chemistry of Materials **24**(5), 774–780 (2011).
[37]S.-W. Lee, K.-S. Lee, J. Ahn, J.-J. Lee, M.-G. Kim, and Y.-B. Shin, "Highly sensitive biosensing using arrays of plasmonic Au nanodisks realized by nanoimprint lithography," ACS Nano **5**(2), 897–904 (2011).
[38]H. J. Park, M.-G. Kang, and L. J. Guo, "Large area high density sub-20 nm SiO_2 nanostructures fabricated by block copolymer template for nanoimprint lithography," ACS Nano **3**(9), 2601–2608 (2009).
[39]W. Wu, M. Hu, F. S. Ou, Z. Li, and R. S. Williams, "Cones fabricated by 3D nanoimprint lithography for highly sensitive surface enhanced Raman spectroscopy," Nanotechnology **21**(25), 255502 (2010).
[40]C. L. Haynes, A. D. McFarland, M. T. Smith, J. C. Hulteen, and R. P. Van Duyne, "Angle-resolved nanosphere lithography: Manipulation of nanoparticle size, shape, and interparticle spacing," The Journal of Physical Chemistry B **106**(8), 1898–1902 (2002).
[41]C. L. Haynes and R. P. Van Duyne, "Nanosphere lithography: A versatile nanofabrication tool for studies of size-dependent nanoparticle optics," The Journal of Physical Chemistry B **105**(24), 5599–5611 (2001).
[42]N. G. Greeneltch, M. G. Blaber, A.-I. Henry, G. C. Schatz, and R. P. Van Duyne, "Immobilized nanorod assemblies: Fabrication and understanding of large area surface-enhanced Raman spectroscopy substrates," Analytical Chemistry **85**(4), 2297–2303 (2013).
[43]X. F. Liu, C. H. Sun, N. C. Linn, B. Jiang, and P. Jiang, "Wafer-scale surface-enhanced Raman scattering substrates with highly reproducible enhancement," J Phys Chem C **113**(33), 14804–14811 (2009).
[44]J.-F. Masson, K. F. Gibson, and A. Provencher-Girard, "Surface-enhanced Raman spectroscopy amplification with film over etched nanospheres," The Journal of Physical Chemistry C **114**(51), 22406–22412 (2010).
[45]C. Wang, W. Ruan, N. Ji, W. Ji, S. Lv, C. Zhao, and B. Zhao, "Preparation of nanoscale Ag semishell array with tunable interparticle distance and its application in surface-enhanced Raman scattering," The Journal of Physical Chemistry C **114**(7), 2886–2890 (2010).
[46]M. S. Niepel, B. Fuhrmann, H. S. Leipner, and T. Groth, "Nanoscaled surface patterns influence adhesion and growth of human dermal fibroblasts," Langmuir **29**(43), 13278–13290 (2013).
[47]A. B. Zrimsek, A.-I. Henry, and R. P. Van Duyne, "Single molecule surface-enhanced Raman spectroscopy without nanogaps," The Journal of Physical Chemistry Letters **4**(19), 3206–3210 (2013).
[48]S. H. Lee, K. C. Bantz, N. C. Lindquist, S.-H. Oh, and C. L. Haynes, "Self-assembled plasmonic nanohole arrays," Langmuir **25**(23), 13685–13693 (2009).
[49]Z. Li, H. Cai, Z. Han, K. Zhang, N. Pan, X. Wang, X. Zhai, and C. Zeng, "Symmetry-dependent plasmonic properties of three-dimensional hybrid metallic nanostructure arrays," The Journal of Physical Chemistry C **116**(33), 17781–17786 (2012).
[50]S. Ye, A. L. Routzahn, and R. L. Carroll, "Fabrication of 3D metal dot arrays by geometrically structured dynamic shadowing lithography," Langmuir **27**(22), 13806–13812 (2011).
[51]E. M. Akinoglu, A. J. Morfa, and M. Giersig, "Understanding anisotropic plasma etching of two-dimensional polystyrene opals for advanced materials fabrication," Langmuir **30**(41), 12354–12361 (2014).
[52]C. Wang, X. Wu, P. Dong, D. Di, and R. Xiao, "Hotspots engineered nanostructure arrays for surface-enhanced Raman scattering by tilted metal deposition," J Nanosci Nanotechno **16**(8), 8374–8379 (2016).
[53]A. Kosiorek, W. Kandulski, P. Chudzinski, K. Kempa, and M. Giersig, "Shadow nanosphere lithography: Simulation and experiment," Nano Letters **4**(7), 1359–1363 (2004).
[54]X. Li, Y. Zhang, Z. X. Shen, and H. J. Fan, "Highly ordered arrays of particle-in-bowl plasmonic nanostructures for surface-enhanced Raman scattering," Small **8**(16), 2548–2554 (2012).
[55]P. Wang, O. Liang, W. Zhang, T. Schroeder, and Y. H. Xie, "Ultra-sensitive graphene-plasmonic hybrid platform for label-free detection," Adv Mater **25**(35), 4918–4924 (2013).
[56]T. H. Lin, N. C. Linn, L. Tarajano, B. Jiang, and P. Jiang, "Electrochemical SERS at periodic metallic nanopyramid arrays," J Phys Chem C **113**(4), 1367–1372 (2009).
[57]C. G. Wang, X. Z. Wu, D. Di, P. T. Dong, R. Xiao, and S. Q. Wang, "Orientation-dependent nanostructure arrays based on anisotropic silicon wet-etching for repeatable surface-enhanced Raman scattering," Nanoscale **8**(8), 4672–4680 (2016).
[58]M. D. Porter, R. J. Lipert, L. M. Siperko, G. Wang, and R. Narayanan, "SERS as a bioassay platform: Fundamentals, design, and applications," Chem Soc Rev **37**(5), 1001–1011 (2008).
[59]H. Chen, Y. Wang, S. Dong, and E. Wang, "An approach for fabricating self-assembled monolayer of Ag nanoparticles on gold as the SERS-active substrate," Spectrochim Acta A Mol Biomol Spectrosc **64**(2), 343–348 (2006).
[60]E. Chung, R. Gao, J. Ko, N. Choi, D. W. Lim, E. K. Lee, S. I. Chang, and J. Choo, "Trace analysis of mercury(ii) ions using aptamer-modified Au/Ag core-shell nanoparticles and SERS spectroscopy in a microdroplet channel," Lab Chip **13**(2), 260–266 (2013).
[61]A. K. Samal, L. Polavarapu, S. Rodal-Cedeira, L. M. Liz-Marzan, J. Perez-Juste, and I. Pastoriza-Santos, "Size tunable Au@Ag core-shell nanoparticles: Synthesis and surface-enhanced Raman scattering properties," Langmuir **29**(48), 15076–15082 (2013).
[62]D. K. Lim, K. S. Jeon, J. H. Hwang, H. Kim, S. Kwon, Y. D. Suh, and J. M. Nam, "Highly uniform and reproducible surface-enhanced Raman scattering from DNA-tailorable nanoparticles with 1-nm interior gap," Nat Nanotechnol **6**(7), 452–460 (2011).
[63]D. K. Lim, K. S. Jeon, H. M. Kim, J. M. Nam, and Y. D. Suh, "Nanogap-engineerable Raman-active nanodumbbells for single-molecule detection," Nat Mater **9**(1), 60–67 (2010).
[64]J. H. Lee, J. M. Nam, K. S. Jeon, D. K. Lim, H. Kim, S. Kwon, H. Lee, and Y. D. Suh, "Tuning and maximizing the single-molecule surface-enhanced Raman scattering from DNA-tethered nanodumbbells," ACS Nano (2012).
[65]H. Deng, X. Li, Q. Peng, X. Wang, J. Chen, and Y. Li, "Monodisperse magnetic single-crystal ferrite microspheres," Angewandte Chemie **117**(18), 2842–2845 (2005).
[66]S. Xuan, F. Wang, Y.-X. J. Wang, J. C. Yu, and K. C.-F. Leung, "Facile synthesis of size-controllable monodispersed ferrite nanospheres," J Mater Chem **20**(24), 5086–5094 (2010).
[67]J. Liu, R. Che, H. Chen, F. Zhang, F. Xia, Q. Wu, and M. Wang, "Microwave absorption enhancement of multifunctional composite microspheres with spinel Fe_3O_4 cores and anatase TiO_2 shells," Small **8**(8), 1214–1221 (2012).
[68]E. Temur, A. Zengin, I. H. Boyaci, F. C. Dudak, H. Torul, and U. Tamer, "Attomole sensitivity of staphylococcal enterotoxin B detection using an aptamer-modified surface-enhanced Raman scattering probe," Anal Chem **84**(24), 10600–10606 (2012).
[69]J. M. Li, W. F. Ma, L. J. You, J. Guo, J. Hu, and C. C. Wang, "Highly sensitive detection of target ssDNA based on SERS liquid chip using suspended magnetic nanospheres as capturing substrates," Langmuir **29**(20), 6147–6155 (2013).
[70]J. Bao, W. Chen, T. Liu, Y. Zhu, P. Jin, L. Wang, J. Liu, Y. Wei, and Y. Li, "Bifunctional Au-Fe_3O_4 nanoparticles for protein separation," ACS Nano **1**(4), 293–298 (2007).
[71]Y. Qiu, D. Deng, Q. Deng, P. Wu, H. Zhang, and C. Cai, "Synthesis of magnetic Fe_3O_4–Au hybrids for sensitive SERS detection of cancer cells at low abundance," J Mater Chem B **3**(22), 4487–4495 (2015).
[72]X. Ji, R. Shao, A. M. Elliott, R. J. Stafford, E. Esparza-Coss, J. A. Bankson, G. Liang, Z.-P. Luo, K. Park, J. T. Markert, and C. Li, "Bifunctional gold nanoshells with a superparamagnetic iron oxide–silica core suitable for both mr imaging and photothermal therapy," J Phys Chem C **111**(17), 6245–6251 (2007).
[73]B. Han, N. Choi, K. H. Kim, D. W. Lim, and J. Choo, "Application of silver-coated magnetic microspheres to a SERS-based optofluidic sensor," J Phys Chem C **115**(14), 6290–6296 (2011).
[74]H. Hu, Z. Wang, L. Pan, S. Zhao, and S. Zhu, "Ag-coated $Fe_3O4@SiO_2$ three-ply composite microspheres: Synthesis, characterization, and application in

detecting melamine with their surface-enhanced Raman scattering," J Phys Chem C **114**(17), 7738–7742 (2010).
[75]J. Li, L. Zheng, H. Cai, W. Sun, M. Shen, G. Zhang, and X. Shi, "Facile one-pot synthesis of Fe_3O_4@Au composite nanoparticles for dual-mode MR/CT imaging applications," ACS Applied Materials & Interfaces **5**(20), 10357–10366 (2013).
[76]K. R. Brown, D. G. Walter, and M. J. Natan, "Seeding of colloidal Au nanoparticle solutions. 2. Improved control of particle size and shape," Chem Mater **12**(2), 306–313 (2000).
[77]J. L. Lyon, D. A. Fleming, M. B. Stone, P. Schiffer, and M. E. Williams, "Synthesis of Fe oxide core/Au shell nanoparticles by iterative hydroxylamine seeding," Nano Lett **4**(4), 719–723 (2004).
[78]X. Zhou, W. Xu, Y. Wang, Q. Kuang, Y. Shi, L. Zhong, and Q. Zhang, "Fabrication of cluster/shell Fe_3O_4/Au nanoparticles and application in protein detection via a SERS method," J Phys Chem C **114**(46), 19607–19613 (2010).
[79]F. Bao, J.-L. Yao, and R.-A. Gu, "Synthesis of magnetic Fe_2O_3/Au core/shell nanoparticles for bioseparation and immunoassay based on surface-enhanced Raman spectroscopy," Langmuir **25**(18), 10782–10787 (2009).
[80]Q. An, M. Yu, Y. Zhang, W. Ma, J. Guo, and C. Wang, "Fe_3O_4@carbon microsphere supported Ag–Au bimetallic nanocrystals with the enhanced catalytic activity and selectivity for the reduction of nitroaromatic compounds," The Journal of Physical Chemistry C **116**(42), 22432–22440 (2012).
[81]F. Xu, K. Cui, Y. Sun, C. Guo, Z. Liu, Y. Zhang, Y. Shi, and Z. Li, "Facile synthesis of urchin-like gold submicrostructures for nonenzymatic glucose sensing," Talanta **82**(5), 1845–1852 (2010).
[82]Z. Gan, A. Zhao, M. Zhang, W. Tao, H. Guo, Q. Gao, R. Mao, and E. Liu, "Controlled synthesis of Au-loaded Fe_3O_4@C composite microspheres with superior SERS detection and catalytic degradation abilities for organic dyes," Dalton Transactions **42**(24), 8597 (2013).
[83]H. Jiang, X. Zeng, Z. Xi, M. Liu, C. Li, Z. Li, L. Jin, Z. Wang, Y. Deng, and N. He, "improvement on controllable fabrication of streptavidin-modified three-layer core–shell Fe_3o_4@SiO_2@Au magnetic nanocomposites with low fluorescence background," Journal of Biomedical Nanotechnology **9**(4), 674–684 (2013).
[84]E. C. Le Ru, E. Blackie, M. Meyer, and P. G. Etchegoin, "Surface enhanced Raman scattering enhancement factors: A comprehensive study," The Journal of Physical Chemistry C **111**(37), 13794–13803 (2007).
[85]Y. Liu, H. Zhou, Z. Hu, G. Yu, D. Yang, and J. Zhao, "Label and label-free based surface-enhanced Raman scattering for pathogen bacteria detection: A review," Biosensors and Bioelectronics **94**, 131–140 (2017).
[86]P. Kubryk, R. Niessner, and N. P. Ivleva, "The origin of the band at around 730 cm^{-1} in the SERS spectra of bacteria: A stable isotope approach," Analyst **141**(10), 2874–2878 (2016).
[87]S. Efrima and L. Zeiri, "Understanding SERS of bacteria," Journal of Raman Spectroscopy **40**(3), 277–288 (2009).
[88]T. T. Liu, Y. H. Lin, C. S. Hung, T. J. Liu, Y. Chen, Y. C. Huang, T. H. Tsai, H. H. Wang, D. W. Wang, J. K. Wang, Y. L. Wang, and C. H. Lin, "A high speed detection platform based on surface-enhanced Raman scattering for monitoring antibiotic-induced chemical changes in bacteria cell wall," PLoS One **4**(5), e5470 (2009).
[89]J. Sundaram, B. Park, Y. Kwon, and K. C. Lawrence, "Surface enhanced Raman scattering (SERS) with biopolymer encapsulated silver nanosubstrates for rapid detection of foodborne pathogens," Int J Food Microbiol **167**(1), 67–73 (2013).
[90]H. Chu, Y. Huang, and Y. Zhao, "Silver nanorod arrays as a surface-enhanced Raman scattering substrate for foodborne pathogenic bacteria detection," Appl Spectrosc **62**(8), 922–931 (2008).
[91]H. Zhou, D. Yang, N. P. Ivleva, N. E. Mircescu, S. Schubert, R. Niessner, A. Wieser, and C. Haisch, "Label-free in situ discrimination of live and dead bacteria by surface-enhanced Raman scattering," Analytical Chemistry **87**(13), 6553–6561 (2015).
[92]P. A. Mosier-Boss, K. C. Sorensen, R. D. George, P. C. Sims, and A. O'Braztsova, "SERS substrates fabricated using ceramic filters for the detection of bacteria: Eliminating the citrate interference," Spectrochim Acta A Mol Biomol Spectrosc **180**, 161–167 (2017).
[93]P. A. Mosier-Boss, K. C. Sorensen, R. D. George, and A. Obraztsova, "SERS substrates fabricated using ceramic filters for the detection of bacteria," Spectrochim Acta A Mol Biomol Spectrosc **153**, 591–598 (2016).
[94]E. Witkowska, T. Szymborski, A. Kaminska, and J. Waluk, "Polymer mat prepared via forcespinning as a SERS platform for immobilization and detection of bacteria from blood plasma," Mater Sci Eng C Mater Biol Appl **71**, 345–350 (2017).
[95]C. Wang, F. Madiyar, C. Yu, and J. Li, "Detection of extremely low concentration waterborne pathogen using a multiplexing self-referencing SERS microfluidic biosensor," J Biol Eng **11**, 9 (2017).
[96]Z. Shan, Q. Wu, X. Wang, Z. Zhou, K. D. Oakes, X. Zhang, Q. Huang, and W. Yang, "Bacteria capture, lysate clearance, and plasmid DNA extraction using pH-sensitive multifunctional magnetic nanoparticles," Analytical Biochemistry **398**(1), 120–122 (2010).
[97]Y.-F. Huang, Y.-F. Wang, and X.-P. Yan, "Amine-functionalized magnetic nanoparticles for rapid capture and removal of bacterial pathogens," Environmental Science & Technology **44**(20), 7908–7913 (2010).
[98]Y. Wang, B. Yan, and L. Chen, "SERS tags: Novel optical nanoprobes for bioanalysis," Chem Rev **113**(3), 1391–1428 (2013).
[99]B. Zhao, J. Shen, S. Chen, D. Wang, F. Li, S. Mathur, S. Song, and C. Fan, "Gold nanostructures encoded by non-fluorescent small molecules in polyA-mediated nanogaps as universal SERS nanotags for recognizing various bioactive molecules," Chem Sci **5**(11), 4460–4466 (2014).
[100]B. H. Jun, M. S. Noh, J. Kim, G. Kim, H. Kang, M. S. Kim, Y. T. Seo, J. Baek, J. H. Kim, J. Park, S. Kim, Y. K. Kim, T. Hyeon, M. H. Cho, D. H. Jeong, and Y. S. Lee, "Multifunctional silver-embedded magnetic nanoparticles as SERS nanoprobes and their applications," Small **6**(1), 119–125 (2010).
[101]A. Abbaspour, F. Norouz-Sarvestani, A. Noori, and N. Soltani, "Aptamer-conjugated silver nanoparticles for electrochemical dual-aptamer-based sandwich detection of staphylococcus aureus," Biosens Bioelectron **68**, 149–155 (2015).
[102]J. Yuan, S. Wu, N. Duan, X. Ma, Y. Xia, J. Chen, Z. Ding, and Z. Wang, "A sensitive gold nanoparticle-based colorimetric aptasensor for Staphylococcus aureus," Talanta **127**, 163–168 (2014).
[103]J. Yuan, Y. Yu, C. Li, X. Ma, Y. Xia, J. Chen, and Z. Wang, "Visual detection and microplate assay for Staphylococcus aureus based on aptamer recognition coupled to tyramine signal amplification," Microchim Acta **181**(3-4), 321–327 (2013).
[104]Y. C. Chang, C. Y. Yang, R. L. Sun, Y. F. Cheng, W. C. Kao, and P. C. Yang, "Rapid single cell detection of Staphylococcus aureus by aptamer-conjugated gold nanoparticles," Sci Rep **3**, 1863 (2013).
[105]N. Duan, S. Wu, C. Zhu, X. Ma, Z. Wang, Y. Yu, and Y. Jiang, "Dual-color upconversion fluorescence and aptamer-functionalized magnetic nanoparticles-based bioassay for the simultaneous detection of Salmonella typhimurium and Staphylococcus aureus," Anal Chim Acta **723**, 1–6 (2012).
[106]J. Li, M. Xu, H. Huang, J. Zhou, E. Abdel-Halimb, J.-R. Zhang, and J.-J. Zhu, "Aptamer-quantum dots conjugates-based ultrasensitive competitive electrochemical cytosensor for the detection of tumor cell," Talanta **85**(4), 2113–2120 (2011).
[107]Y. J. Sung, H. J. Suk, H. Y. Sung, T. Li, H. Poo, and M. G. Kim, "Novel antibody/gold nanoparticle/magnetic nanoparticle nanocomposites for immunomagnetic separation and rapid colorimetric detection of Staphylococcus aureus in milk," Biosens Bioelectron **43**, 432–439 (2013).
[108]A. K. Singh, D. Senapati, S. Wang, J. Griffin, A. Neely, P. Candice, K. M. Naylor, B. Varisli, J. R. Kalluri, and P. C. Ray, "Gold nanorod based selective identification of Escherichia coli bacteria using two-photon Rayleigh scattering spectroscopy," ACS Nano **3**(7), 1906–1912 (2009).
[109]V. Escamilla-Gómez, S. Campuzano, M. Pedrero, and J. M. Pingarrón, "Immunosensor for the determination of Staphylococcus aureus using a

tyrosinase–mercaptopropionic acid modified electrode as an amperometric transducer," Anal Bioanal Chem **391**(3), 837–845 (2008).
[110]T. Majumdar, R. Chakraborty, and U. Raychaudhuri, "Development of PEI-GA modified antibody based sensor for the detection of S. aureus in food samples," Food Bioscience **4**, 38–45 (2013).
[111]G. A. Zelada-Guillen, J. L. Sebastian-Avila, P. Blondeau, J. Riu, and F. X. Rius, "Label-free detection of Staphylococcus aureus in skin using real-time potentiometric biosensors based on carbon nanotubes and aptamers," Biosens Bioelectron **31**(1), 226–232 (2012).
[112]U. Tamer, İ. H. Boyacı, E. Temur, A. Zengin, İ. Dincer, and Y. Elerman, "Fabrication of magnetic gold nanorod particles for immunomagnetic separation and SERS application," J Nanopart Res **13**(8), 3167–3176 (2011).
[113]C. Wang, J. Wang, M. Li, X. Qu, K. Zhang, Z. Rong, R. Xiao, and S. Wang, "A rapid SERS method for label-free bacteria detection using polyethylenimine-modified Au-coated magnetic microspheres and Au@Ag nanoparticles," Analyst **141**(22), 6226–6238 (2016).
[114]J. Wang, X. Wu, C. Wang, N. Shao, P. Dong, R. Xiao, and S. Wang, "Magnetically assisted surface-enhanced Raman spectroscopy for the detection of Staphylococcus aureus based on aptamer recognition," ACS Applied Materials & Interfaces **7**(37), 20919–20929 (2015).
[115]J. Wang, X. Wu, C. Wang, Z. Rong, H. Ding, H. Li, S. Li, N. Shao, P. Dong, R. Xiao, and S. Wang, "Facile synthesis of Au-coated magnetic nanoparticles and their application in bacteria detection via a SERS method," ACS Appl Mater Interfaces **8**(31), 19958–19967 (2016).